Mechanics and Mechanical Engineering
Vol. 21, No. 3 (2017) 467–483

Study of Void Growth and Coalescence in HDPE Material: A Numerical Investigation Using Computational Voided Cells

M. N. D. Cherief
M. Benguediab
M. Elmeguenni
University Djillali Liabes of Sidi Bel Abbes
BP 89 City Ben Mhidi, Sidi Bel Abbes 22000, Algeria
nadhir.cherief@univ-sba.dz
benguediabm@gmail.com
elmeguennimohamed@yahoo.fr

A. Reffas
Department of Engineering Mechanics
University of Sciences and Technology of Oran
El Mnaouar, BP 1505, Bir El Djir 31000, Algeria
reffas_ahmed@yahoo.fr

Received (10 March 2017)
Revised (25 April 2017)
Accepted (18 June 2017)

This paper presents a study about the effects of initial porosity and stress triaxiality on void growth and coalescence in High–density polyethylene (HDPE) material. Two approaches are used to modulate the representative material volume: The first one is a unit cell with a spherical void at the center (Voided cell model), and the second is a unit cell containing the same void fraction of volume and obeying to the constitutive relation of Gurson–Tvergaard–Needelman (GTN model). Detailed analyses of finite element gave us: the equivalent stress–strain response, the void growth and coalescence behavior of the representative material volume. Results show that the stress triaxiality and the initial void volume fraction are strongly effective and depended on.

Keywords: void growth, coalescence, damage, HDPE, polymer, triaxiality.

1. Introduction

The understanding of the intrinsic mechanical behavior of semi crystalline polymers is of a prime importance in the design of components made of it because of its frequent use nowadays in engineering components that may lead to experience complex mechanical loadings. These few past decades, considerable attention has been focused on the plastic deformation of polymers and it has been widely investigated by [1–5]. As known the parameters that influence solid polymers the most

are: The temperature, the strain rate, the strain, and the type of loading conditions, which means the stress triaxiality. Some experimental devices were proposed in order to define the effects of stress triaxiality on solid polymer's mechanical properties (e.g. yield strength or ultimate properties) by [6, 7]. These systems are as complex as it seems very difficult to obtain any intrinsic stress-strain curves.

Gurson and Sànchez et al [8, 9] proposed many phenomenological laws and other studies have been based only on the mechanical behavior in largescale deformation [10–14]. It is now recognized that three successive courses that are nucleation (or germination) of the cavity, their growth, and coalescence of voids at a later stage of the deformation lead to the damage of ductile materials like polymers.

In the same time, and in order to understand the mechanisms of voids growth and coalescence and to develop micro-mechanical models for better describing the ductile fracture of polymers, research efforts have been devoted. The wellknown micromechanical model proposed by Gurson [8] and phenomenologically extended by [15–17] for which the damage is expressed as the porosity due to spherical micro voids is particularly well suited for modeling porous ductile metals. The understanding of the influence of porosity in ductile materials has been ensured by detailed micromechanical analysis for characteristic cell models with known porosity.

Therefore, accounting for void coalescence in constitutive damage models is generally considered as obligatory to describe the fracture of ductile solids [17]. Most of the several models of void coalescence proposed by [18, 19] are dedicated to coalescence by internal necking.

In contrast, and in order to investigate the behavior of porous solids, finite element cell computations are commonly used, see e.g. in [16, 20–24]. Such simulations proved to be an important tool in allowing a better understanding of the micro mechanisms of failure in ductile media even though it is restricted to materials with periodic microstructure.

This paper describes an application of a finite element analysis in the prediction of ductile fracture of the standard axisymmetric cell model which has been employed by several investigators in early studies [15, 16, 20, 25]. The analyses were based on the cell model with special boundary conditions allowing a relatively simple appraisal of a full three-dimensional array of voids, without having to solve the full 3D numerical problem. Detailed fully three-dimensional computations were also performed in [26–29]. The cell model used in these investigations, is a cylindrical representative volume element (RVE) containing initially a spherical void subjected to an axisymmetric loading, generally with predominant axial stress. Additionally, during the whole process of deformation of the cell model the overall stress triaxiality is kept constant. This geometry was in fact an approximation of a cylindrical volume with some hexagonal basis, which can be considered as an elementary cell in a periodically voided material. Direct comparisons are made between the numerical obtained stress-strain and void growth response of the voided cell model and cell model using GTN constitutive relation.

The polymer investigated in this work, is the High-density polyethylene (HDPE). It is one of the most used polymers in the world, for its large variety of industrial applications, in particular for packaging industries of Building and Public Works. The HDPE is a thermoplastic polymer with good strength, toughness and resistance to acids as well as aging.

2. Material and numerical methods

2.1. *Material characteristics*

A model type of HDPE material characterizes the void matrix material. The physical properties are: density 0.9 g/cm^3, Melt–Mass–Flow = 1.2 g/10 min, Molecular–Weight 310000, Glass Transition Temperature = 84^{o}C, Melting Point = 180^{o}C, and crystallinity index $\approx$ 66 %. The true strain at break is around 250%. The Young's modulus E obtained from the initial slope is equal to 850 MPa. The yield stress σy, defined as the intersection point between the tangent at the origin and the tangent of the plateau before hardening, is equal to 25 MPa.

2.2. *Computational Unit Cell Model*

Axisymmetric geometries are efficient and allow for a good estimation of damage evolution and fracture strains that is why cell studies have focused on their use [18, 20, 25, 29]. It should be emphasized that axisymmetric models provide a lower, and therefore, more conservative estimate for damage evolution and the fracture strain (coalescence) than their 3D counterparts.

Large-strain computations of void growth and coalescence have been carried out in the finite element code. An axisymmetric model of a cylindrical cell containing a single initially spherical void at its center is considered. See Fig. 1.

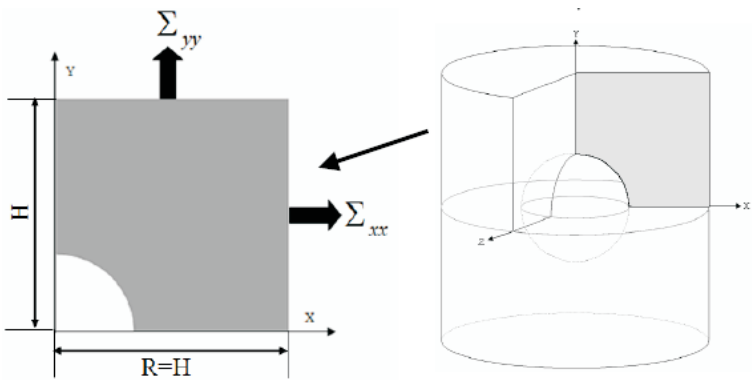

Figure 1 Micromechanical modeling from unit cells and 2D approximation

The quantities calculated locally at each point of the cell are of a microscopic scale. The macroscopic quantities correspond to the mean of the volume of the cell. Due to the symmetries of geometry and loading, only one quarter of the cell is considered. A load is applied to these two outer faces.

The axial macroscopic constraints Σ_{yy} and radial Σ_{xx} are formulated as follows:

$$\begin{aligned} \Sigma_{xx} &= \frac{F_x}{4\pi HR} \\ \Sigma_{yy} &= \frac{F_y}{\pi R^2} \end{aligned} \tag{1}$$

where F_x and F_y are respectively the reactions at the level of the lateral face and the base of the REV (Representative Elementary Volume). H and R are respectively the half height and the radius of the unit cell. Then the average macroscopic constraints Σ_m and equivalent Σ_{eq} are given in the axisymmetric case by:

$$\begin{aligned} \Sigma_m &= \frac{1}{3}\left(2\Sigma_{xx} + \Sigma_{yy}\right) \\ \Sigma_{eq} &= |\Sigma_{yy} - \Sigma_{xx}| \end{aligned} \tag{2}$$

The axial macroscopic deformations E_{yy}, radial E_{xx} and equivalentE_{eq} are defined by the following expressions:

$$\begin{aligned} E_{xx} &= \ln\left(\frac{R + u_{xx}}{R}\right) \\ E_{yy} &= \ln\left(\frac{H + u_{yy}}{H}\right) \\ \Sigma_{eq} &= \frac{2}{3}\left|E_{yy} - E_{xx}\right| \end{aligned} \tag{3}$$

where u_{xx} and u_{yy} are the components of the displacement in the x and y directions. There is two ways to calculate the volume fraction of voids, either the numerical integration along the points of the vacuum surface, or the use of the approximate formula proposed by Koplik and Needleman [20].

$$f = 1 - (1 - f_0)\left[1 + \frac{3\,(1-2\nu)}{E}\Sigma_m\right]\frac{V_{tot}^0}{V_{tot}} \tag{4}$$

where V_{tot}^0, V_{tot}, f_0 and f denote respectively the initial and final volumes and the initial and final porosities of the cell. One of the difficulties of the numerical study of a REV using the model of the elementary cell is the maintenance of the triaxiality to a constant value during loading. In the case of an implicit calculation, the RIKS method can be advantageously exploited to satisfy this condition.

We present in the following a technique of explicit cell computation proposed by Siad et al. [30] allowing to maintain a constant triaxiality during the deformation. This constraint is satisfied after a number of calculations. The loading is applied this time via a displacement fixed on the upper corner of the cell as depicted in Fig. 2.

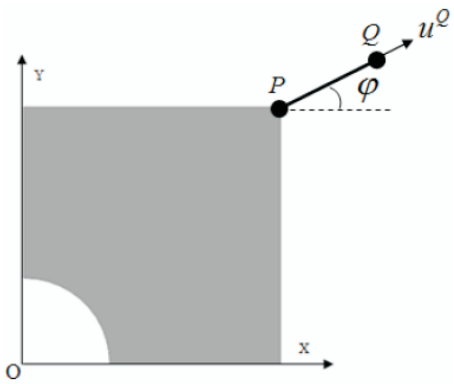

Figure 2 Loading of the unit cell using a linear stiff elastic truss

The axisymmetric loadings of the unit cell are for all numerical simulations considered with dominant axial traction (along the y-axis) and a constant triaxiality T equal to (0,33; 0,44; 0,6; 1).
There are few techniques in the cell calculations, which make it possible to maintain the constant triaxiality during the loading. The RIKS algorithm is simple to use in the case considered here but nonetheless efficient [31]. However, its use cannot be coupled with an explicit integration approach due to the role of the time parameter. On the other hand, in its current version, Abaqus standard (Implicit analysis) excludes the coalescence parameters in the Gurson potential. In contrast, Abaqus/Explicit allows us to do this. Fig. 2 shows schematically a cell loading which allows, by successive adjustments during the computation, to tend towards the situation where the triaxiality is kept constant during its evolution. An elastic bar PQ of initial length L_0, of constant cross section S_b and inclined by an initial angle φ_0 relative to the horizontal, is fixed to the upper right corner P of the cell. The cell is loaded by means of the bar PQ for which the position in the plane $(x,\ y)$ of its end Q is imposed so as to maintain the triaxiality at the desired value. An adequate displacement u^Q of its end Q is imposed. We denote by u^P and u^Q the displacements of the extremities P and Q whose decompositions along the directions $(x,\ y)$ are written as:

$$\begin{aligned} u^P &= u_x^P e_x + u_y^P e_y \\ u^Q &= u_x^Q e_x + u_y^Q e_y \end{aligned} \tag{5}$$

The position of the end Q is then given by:

$$\begin{aligned} X^Q &= R_0 + u_x^P + L\cos\varphi \\ Y^Q &= H_0 + u_y^P + L\sin\varphi \end{aligned} \tag{6}$$

where L is the current length of the bar and the angle φ is such that:

$$\begin{aligned} \cos\varphi &= \cos\varphi_0 - \frac{u_x^Q - u_x^P}{L_0} \\ \sin\varphi &= \sin\varphi_0 - \frac{u_y^Q - u_y^P}{L_0} \end{aligned} \tag{7}$$

with φ_0 the value of the angle φ corresponding to $u^P = u^Q = 0$. The current value of φ can also be calculated by:

$$\tan\varphi = \frac{Y^Q - Y^P}{X^Q - X^P} = \frac{L_0 \sin\varphi_0 + u_y^Q - u_y^P}{L_0 \cos\varphi_0 + u_x^Q - u_x^P} \tag{8}$$

We denote by Σ_r axial stress acting on the bar PQ. The main and equivalent macroscopic constraints acting on the cell are given by:

$$\begin{aligned} \Sigma_{xx} &= \frac{\Sigma_r S_r \cos\varphi}{2\pi\left(R_0 + u_x^P\right)\left(H_0 + u_y^P\right)} \\ \Sigma_{yy} &= \frac{\Sigma_r S_r \sin\varphi}{\pi\left(R_0 + u_x^P\right)^2} \\ \Sigma_{eq} &= |\Sigma_{yy} - \Sigma_{xx}| \end{aligned} \tag{9}$$

By means of a first approximation deduced from the hypothesis of invariance of the global volume of the cell during loading, it is possible to establish a relation between the Triaxiality T, the angle φ and the vertical displacement of the point P. Indeed, by definition we have:

$$T = \frac{\Sigma_m}{\Sigma_{eq}} = \frac{1}{3}\left(\frac{\Sigma_{yy} + 2\Sigma_{xx}}{|\Sigma_{yy} + \Sigma_{xx}|}\right) = \frac{1}{3}\left(\frac{1 + 2\alpha}{|1 - \alpha|}\right) \tag{10}$$

with $\alpha = \Sigma_{xx}/\Sigma_{yy}$.
The substitution of equation (IV.9) in the expression of α leads to:

$$\alpha = \frac{1}{2}\frac{1}{\tan\varphi}\frac{\left(R_0 + u_x^P\right)}{\left(H_0 + u_Y^P\right)} = \frac{1}{2}\frac{L_0\cos\varphi_0 + u_x^Q - u_x^P\left(R_0 + u_x^P\right)}{L_0\sin\varphi_0 + u_y^Q - u_y^P\left(H_0 + u_y^P\right)} \tag{11}$$

Moreover, in the absence of porosity, Koplik and Needleman [20] stipulated that, due to Poisson's effect, the overall volume remains constant throughout the loading process. We accept, as a first approximation, the validity of this hypothesis for a porous matrix at least at the beginning of the loading of the cell. In this circumstance, the components satisfy the relation:

$$R_0^2 H_0 = \left(R_0 + u_x^P\right)^2\left(H_0 + u_y^P\right) \tag{12}$$

That expresses explicitly u_x^P in function of u_y^P as we have:

$$u_x^P = u_x^P\left(u_y^P\right) = R_0\left[\left(\frac{H_0}{H_0 + u_y^P}\right)^{1/2} - 1\right] \tag{13}$$

The transfer of equation (12) into equation (6) leads to

$$\begin{aligned} X^Q &= \frac{R_0\sqrt{H_0}}{\left(H_0+u_y^P\right)^{1/2}} + L\cos\varphi \\ Y^Q &= \left(H_0+u_y^P\right) + L\sin\varphi \end{aligned} \tag{14}$$

Therefore:

$$\begin{aligned} u_x^Q &= R_0\sqrt{\frac{H_0}{H_0+u_y^P}} + L\cos\varphi - (R_0 + L_0\cos\varphi_0) \\ u_y^Q &= \left(H_0+u_y^P\right) + L\sin\varphi - (H_0 + L_0\sin\varphi_0) \end{aligned} \tag{15}$$

During the loading of the cell, the components of the displacement of the point P, the triaxiality T through the parameter α and the angle φ are linked by the relation:

$$\tan\varphi = \frac{1}{2\alpha}\left(\frac{R_0+u_x^P}{H_0+u_y^P}\right) = \frac{1}{2\alpha}\left(\frac{R_0\sqrt{H_0}}{\left(H_0+u_y^P\right)^{3/2}}\right) \tag{16}$$

Thus, the initial value φ_0 is fixed by expected triaxiality (parameter α) and the geometry of the outer contour of the cell (H_0 and R_0) through the relation

$$\tan\varphi_0 = \frac{1}{2\alpha}\left(\frac{R_0}{H_0}\right) \tag{17}$$

In order to analyze the behavior of a porous HDPE cell, a single spherical cavity is placed at the center of the latter. The volume fraction of voids f is equal to the ratio V_f/V, V is the volume of the whole cell and V_f that of the vacuum. The dimensions of the cell are such that $R_0 = H_0 = 1\ mm$. The initial volume fraction of voids makes it possible to estimate the initial radius of the cavity in the unit cell. In order to analyze the influence of the triaxiality of the stresses T and the volume fraction of voids f, cells with different initial porosities f_0 (1%, 5% and 10%) were considered and stressed under different triaxialities T.

2.3. *GTN constitutive model*

Ductile fracture is associated with plastic instability characterized by nucleation, growth, and coalescence of voids. The original Gurson model [8] and some other developed models by [32,33] take into consideration the effect of micro voids on plastic performance but only in condition that hydrostatic stress in length affects the yield surface while we suppose that the yielding is independent of the hydrostatic stress as for the classical plasticity theory. The GTN damage model can be described as the following:

$$f = \left(\frac{q}{\overline{s}_m}\right) + 2q_1 f^*\cosh\left(-\frac{3q_2 p}{2\overline{s}_m}\right) - (1+q_3 f^{*2}) \tag{18}$$

where $q = \sqrt{\frac{2}{3} S_{ij} S_{ij}}$ is the macroscopic von Mises equivalent stress, $p = \frac{1}{3}\sigma_{kk}$ is the hydrostatic stress, $S_{ij} = \sigma_{ij} - \frac{1}{3}\sigma_{kk}\delta_{ij}$ is the deviatoric components of the Cauchy stress, δ_{ij} is the Kronecker delta, and σ_m is the equivalent stress of the matrix material; f^* denotes the total effective void volume fraction which accounts for the decrease of the materials stress-carrying capability due to void coalescence[34]. The fitting coefficients q_1, q_2, and q_3 introduced by [15,16] stand for void interaction effects, and normally, $q_1 = 1.5$ and $q_3 = q_1^2$. When all the three fitting parameters equal to 1, the GTN model reduces to the original Gurson model.

Based on the principle of the equivalent plastic work, we can obtain the matrix equivalent plastic strain rate from the microscopic view as follows:

$$\begin{aligned} \sigma : \dot{\varepsilon}^p &= (1-f)\,\bar{\sigma}_m . \dot{\bar{\varepsilon}}_m^{pl} \\ \dot{\bar{\varepsilon}}_m^{pl} &= \frac{\sigma : \dot{\varepsilon}^p}{(1-f)\,\bar{\sigma}_m} \end{aligned} \tag{19}$$

Here, $\dot{\bar{\varepsilon}}_m^{pl}$ is the accumulated equivalent plastic strain rate of the matrix material, $\dot{\varepsilon}^p$ is the macroscopic plastic strain rate, and f is the void volume fraction.

The modified void volume fraction f^* used in the GTN damage model is a piecewise linear function of f and can be defined as in [17].

$$f^* = \begin{cases} f & f \le f_c \\ f_c + \frac{1/q_1 - f_c}{f_F - F_c}(f - f_c) & f_c < f \le f_F \\ 1/q_1 & f > f_F \end{cases} \tag{20}$$

where fc is the initial void volume fraction when void coalescence starts and f_F represents the value of void volume fraction at final fracture. The variation in void volume fraction f depends on growth of pre-existent voids and nucleation of new voids. The rate form relation between them can be expressed as $\dot{f} = \dot{f}_{growth} + \dot{f}_{nucleation}$. Assuming that the matrix material is incompressible, the void volume fraction rate from growth of existing voids is believed to be related to the macroscopic plastic volume and can be represented by:

$$\dot{f}_{growth} = (1-f)\,\dot{\varepsilon}^p : I \tag{21}$$

where I is the second-order unit tensor. In this work, we assume that the void nucleation is strain induced and we adopt the plastic strain controlled nucleation rule by chu and Needleman [35]. Therefore, the void volume fraction rate from new void nucleation can be expressed as:

$$\dot{f}_{nucleation} = A\dot{\bar{\varepsilon}}_m^{pl} = \frac{f_N}{S_N\sqrt{2\pi}} \exp\left[-\frac{1}{2}\left(\frac{\bar{\varepsilon}_m^{pl} - \varepsilon_N}{S_N}\right)^2\right] \dot{\bar{\varepsilon}}_m^{pl} \tag{22}$$

where f_N is the volume fraction of nucleating particles, ε_N is the mean equivalent plastic strain when voids nucleate, and S_N is the corresponding standard deviation.

3. Results and discussion

A finite element program that uses a finite strain has been used in the numerical analyzes. The RVE considered in this study has an equal initial length with the initial radius of the cell. We only needed to modulate one quarter of the region because of the symmetry. We also used a typical finite element mesh in the calculation that is presented in the Fig. 3.

We succeed to reproduce the results of macroscopic stress–strain behavior, plastic deformation and evolution of the void volume fraction of a voided cell initially put forth by Koplik and Needleman [20] by applying the numerical procedures presented.

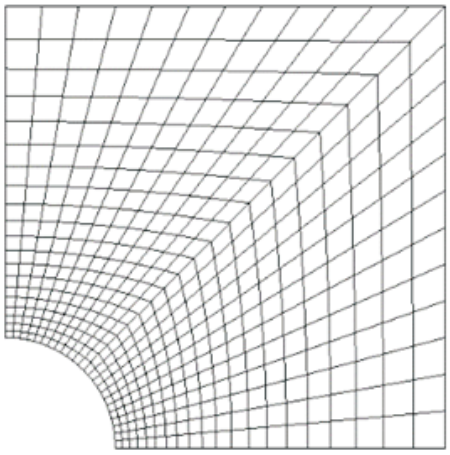

Figure 3 Typical finite element mesh in the calculation

This latter allows the validation of our numerical implementation. Here the conjoint influence of stress triaxiality and initial void volume fraction on void growth and coalescence is examined.

Three initial void volume fractions, $f_0 = 0, 01, 0.05, 0.1$ and four different triaxiality levels ranging between T = 0,33 and 1 (The values of f_0 and T chosen cover the range of initial porosity and stress triaxiality used in common structural applications).

Fig. 4, Fig. 5 and Fig. 6 show the influence of the triaxialities of the stresses on the response of the unit cell and on the GTN model for different initial porosity. Two phases are highlighted; Increase of the stress up to a maximum then a monotonous decrease. Moreover, it is clear that the different phases of the law of behavior are affected by the volume fraction of voids imposed initially. In particular, the higher the initial porosity, the lower the plastic flow limit, the structural hardening and the maximum stress. Furthermore, by comparing Figures 4, 5 and 6, it appears that the effect of the initial porosity on these different phases decreases with the decrease in the triaxiality of the stresses for voided cell and the material element obeying the GTN constitutive relation. It should be noted that the plastic instability leading

to the sudden drop in stress occurring at the end of the deformation process could be attributed to the phenomenon of coalescence due to the ligature of the matrix ligament of the unit cell. The stress drop rapidity follows the initial vacuum rate imposed on the cell. The rate of void growth is affected by f_0. Benzerga and Leblond [36] show that the rate of void growth decreases, and therefore the strain to coalescence increases, with decreasing f_0.

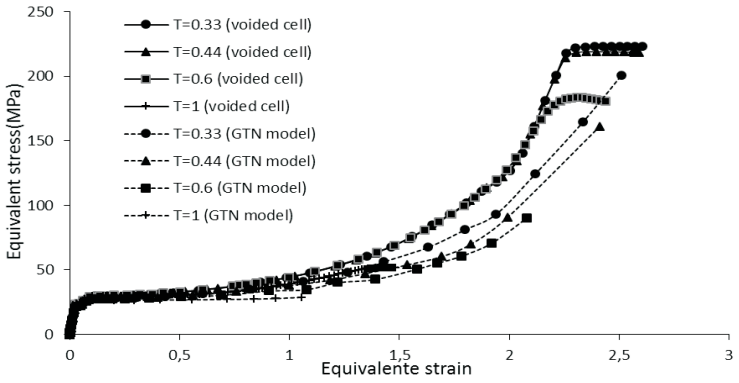

Figure 4 Equivalent stress versus equivalent strain for f_0 =1%

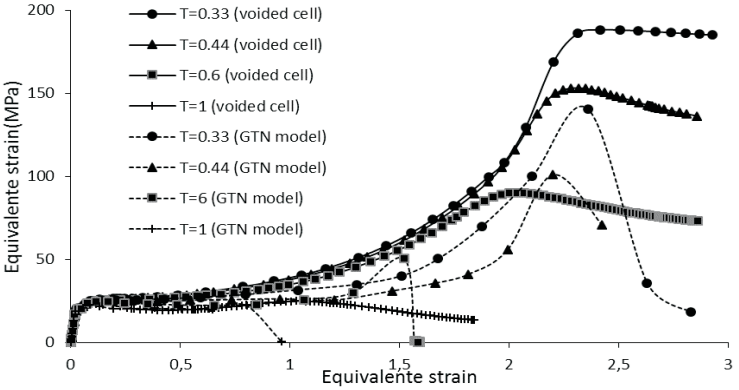

Figure 5 Equivalent stress versus equivalent strain for f_0 =5%

Fig. 7, Fig. 8 and Fig. 9 show the variations of the volumetric strain as a function of the equivalent strain for voided cell and the material element obeying the GTN constitutive relation. We observe that the volume deformation is very low in the elastic part (volume deformation due to the effect of the Poisson's coefficient) and then begins to increase from the beginning of the plasticity at first moderately pedantic the growth phase and then abruptly during the period of coalescence.

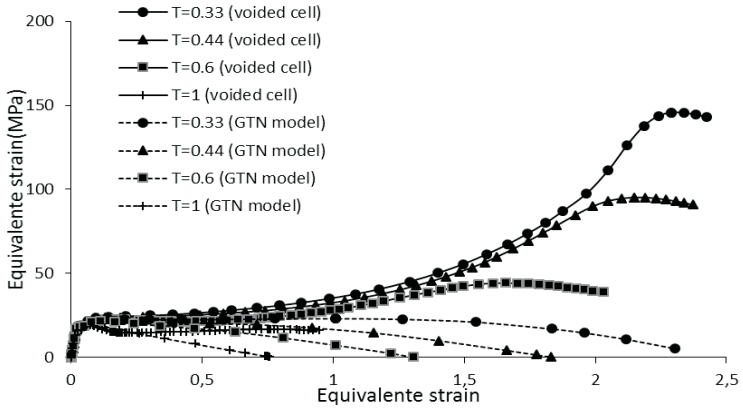

Figure 6 Equivalent stress versus equivalent strain for f_0 =10%

Moreover, the increase of the initial volume fraction of voids implies greater volume deformation which takes an important part of the total deformation. The general trend is similar. However, the instability phase is more pronounced for low volume fractions of vacuum and / or low triaxialities of the stresses.

We observe for the three triaxialities ($T = 0.33,\ T = 0.44,\ T = 0.6$) a very good correlation of the responses with the GTN model and the unitary cell for $f_0 = 0.1$ and $f_0 = 0.05$. During the stage of growth of the cavities, while the stress increases regularly as a function of the deformation, the volume deformation evolves only slowly to a critical value which corresponds to the beginning of coalescence where the material completely loses its rigidity.

However, the volume deformation does not increase with the same tendencies. This can be attributed to the effect of stress triaxiality, which controls the rate of growth of voids. Let us note finally that one of the advantages of the simulation with a GTN model is that we can predict the behavior of the HDPE in its entirety and until its rupture, which means until the material can no longer support the Load.

The analysis of the stress and strain fields inside several void cells has shown that voids start interacting with each other well before the onset of void coalescence. Fig. 10 and fig. 11 compare the critical equivalent stress and strain obtained at the moment of the coalescence as a function of the triaxiality for the different porosities in all cases. In general, stress triaxiality has a negative effect on the coalescence. It is interesting to observe that the void have a strong influence on the reduction of the coalescence.

As shown in Fig. 11, critical deformation evolves non-linearly with the constrained triaxiality and this takes place whatever the initial porosity imposed for voided cell and the material element obeying the GTN constitutive model. So, the effect of triaxiality on the critical stress is marked by an evolution that seems rather non-linear.

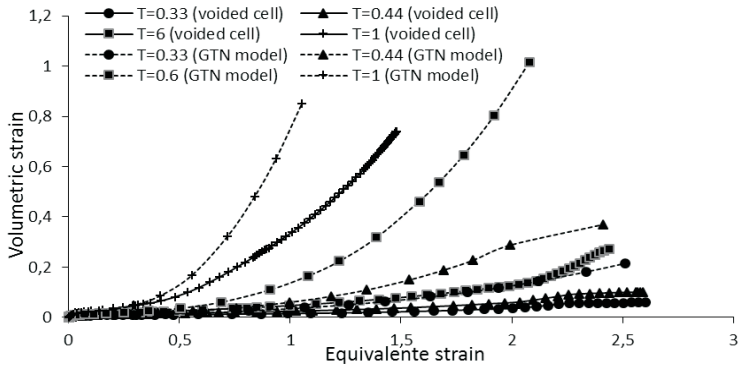

Figure 7 Void volume fraction versus equivalent strain for f_0=1%

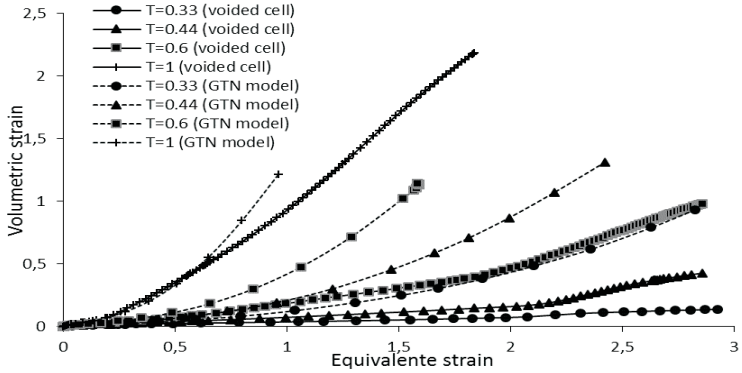

Figure 8 oid volume fraction versus equivalent strain for f_0=5%

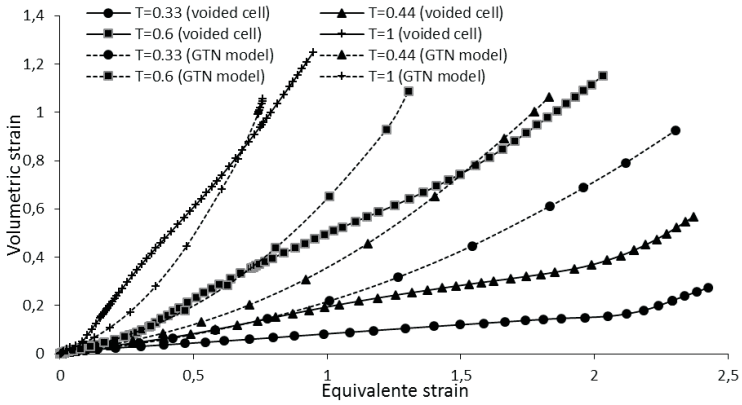

Figure 9 Void volume fraction versus equivalent strain for f_0=10%

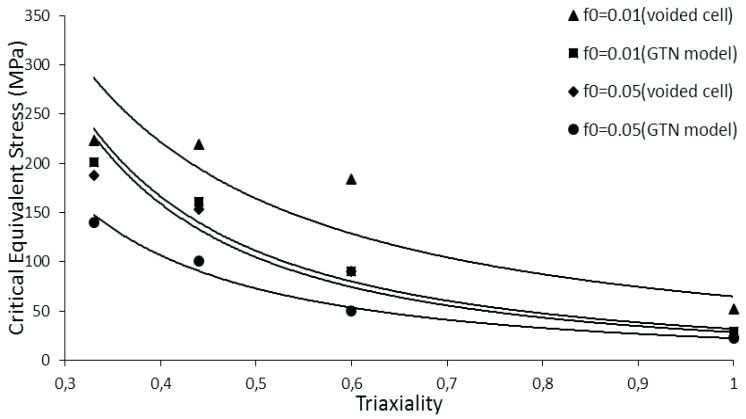

Figure 10 Critical equivalent stress versus triaxiality

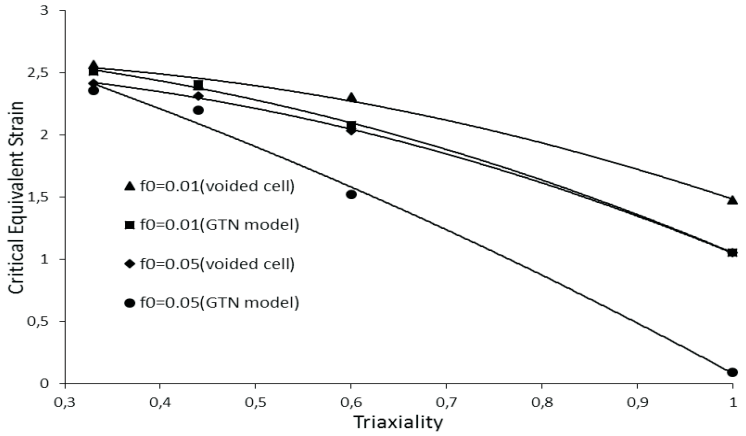

Figure 11 Critical equivalent strain versus triaxiality

As frequently mentioned in the literature [20, 37], the critical porosity at the onset of coalescence significantly varies with T. At low or intermediate stress triaxiality these variations don't allow an accurate constant critical porosity criterion. However, at large stress triaxiality void growth rates are high enough such that the prediction of strain at coalescence based on a constant critical porosity may provide a reasonable approximation.

Fig. 12 plots the critical volume fraction as a function of stress triaxiality for different initial void volume fractions considered. As we can see, an increase in stress triaxiality results in an increase in the critical void volume fraction. For

a fixed stress triaxiality value fc increases significantly with f_0. Similar results have been reported by [18, 38, 39]. The results show that the GTN model allows us to faithfully reproduce the intrinsic macroscopic mechanical behavior (law of behavior and volume variation) of the HDPE, until it breaks.

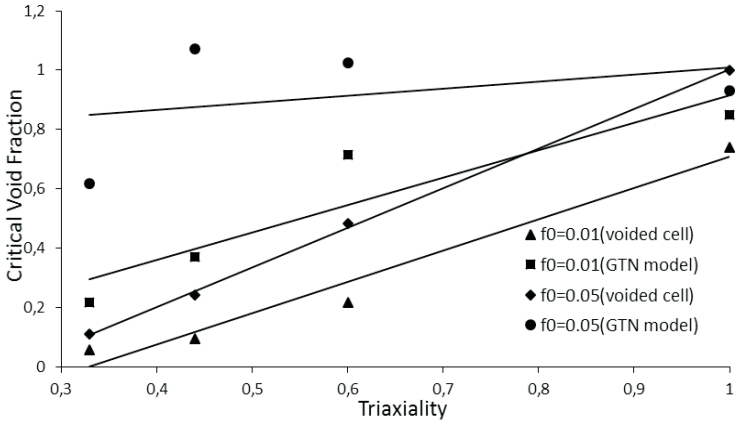

Figure 12 Critical void fraction versus triaxiality

4. Conclusions

We have presented results of calculations on unit cells in order to study the porosity's effects on the global response of HDPE, for the usual stress–strain response and for the plastic volume variation as well. The results have also revealed the effect of triaxiality on global behavior. Based on this study, we can affirm that predictions give promising results. On the other hand, if the triaxiality is maintained constant in the case of numerical simulations, this condition is not verified beyond the plastic limit for axisymmetric specimens, so calculations on porous cell show the interest of taking into account damage in the constitutive law (GTN). For the lowest initial porosity imposed on the unit cell, we can observe a good correlation of the predictions with the results for the large deformations where a greater or less difference appears in the phase of hardening between the curves of the porous unitary cells and the GTN unitary cells. These differences are due to the initial porosity (arbitrarily set at a minimum of 1%). The final break of the material (void coalescence) is assumed to occur when the porosity reaches a critical value. The deformations and the critical stresses decrease nonlinearly as the triaxiality increases, whichever is the considered case. However, the effect is more marked in deformation than in stress.

This work has for an objective the examination of the relevance of models derived from the ductile mechanics damage by the growth of voids (coupling plasticity and damage) in order to predict the mechanical behavior and the damage of the HDPE (until it reaches break) also its evolution during the loading for given solicitations.

References

[1] **Schultz, J. M.**: Microstructural aspects of failure in semicrystalline polymers, *Polymer Engineering and Science*, 24, 770–785, **1984.**

[2] **Joy, J. C., José, A. A., Maria, A. P., and Alexander, P.**: Chain Entanglements and Mechanical Behavior of High Density Polyethylene, *ASEM Journal of Engineering Materials and Tecnoogy*, 132, 1, 011016-011016-7, **2009.**

[3] **Ellyin and Zihui, X.**: Nonlinear Viscoelastic Constitutive Model for Thermoset Polmers, *ASEM Journal of Engineering Materials and Technology*, 128, 4, 579-585, **2006.**

[4] **Benaoumeur, A., and Ali, M.**: Analysis of plastic deformation of semi-crystalline polymers during ecae process using 135° die, *Review Journal of Theoretical and Applied Mechanics*, 54, 5, 263-275, **2016.**

[5] **Jeridia, M., Laiarinandrasanab, L., Saïa, K.**: Comparative study of continuum damage mechanics and Mechanics of Porous Media based on multi-mechanism model on Polyamide 6 semi-crystalline polymer, *International Journal of Solids and Structures*, 53, 12–27, **2015.**

[6] **Liu, Z. G., Wong, W. H., and Guo, T. F.**: Void behaviors from low to high triaxialities: Transition from void collapse to void coalescence, *International Journal of Plasticity*, 84, 183–202, **2016.**

[7] **Chena, F., Gateaa, S., Oua, H., Lub, B., and Longc, H.**: Fracture characteristics of PEEK at various stress triaxialities, *Journal of the Mechanical Behavior of Biomedical Materials*, 64, 173–186, **2016.**

[8] **Gurson, A. L.**: Continuum theory of ductile rupture by void nucleation and growth: Part-I–Yield criteria and flow rules for porous ductile media, *ASEM Journal of Engineering Materials and Technology*, 99, 1, 2-15, **1977.**

[9] **Sànchez, P. J., Huespe, A. E., and Oliver, J.**: On some topics for the numerical simulation of ductile fracture, *International Journal of Plasticity*, 24, 6, 1008-1038, **2008.**

[10] **Zairi, F., Nait-Abdelaziz, M., Woznica, K., and Gloaguen, J. M.**: Elasto-viscoplastic constitutive equations for the description of glassy polymers behavior at constant strain rate, *ASEM Journal of Engineering Materials and Technology*, 129, 1, 29-35, **2007.**

[11] **Rashid, K. A., Ardeshir, H. T., and Masoud, K. D.**: Application of a large deformation nonlinear viscoelastic viscoplastic viscodamage constitutive model to polymers and their composites, *International Journal of Damage Mechanics*, 24, 2, 198–244, **2015.**

[12] **Zairi, F., Nait-Abdelaziz, M., Gloaguen, J. M., and Lefebvre.:** A physically based constitutive model for anisotropic damage in rubber toughened glassy polymers during finite deformation, *International Journal of Plasticity*, 27, 1, 25–51, **2011.**

[13] **Mulliken, A. D., and Boyce, M. C.**: Mechanics of the rate-dependent elastic–plastic deformation of glassy polymers from low to high strain rates, *International Journal of Solids and Structures*, 43, 5, 1331–1356, **2006.**

[14] **Richeton, J., Ahzi, S., Vecchio, K. S., Jiang, F. C., and Makradi, A.**: Modeling and validation of the large deformation inelastic response of amorphous polymers over a wide range of temperatures and strain rates, *International Journal of Solids and Structures*, 44, 4, 7938–7954, **2007.**

[15] **Tvergaard, V.**: Influence of voids on shear bands instabilities under plane strain conditions, *International Journal of Fracture*, 17, 389–407, **1981.**

[16] **Tvergaard, V.**: On localization in ductile materials containing spherical voids, *International Journal of Fracture*, 18, 237–52, **1982.**

[17] **Tvergaard, V., and Needleman A.**: Analysis of the cup-cone fracture in a round tensile bar, *Acta Metallurgica*, 32, 157–69, **1984.**

[18] **Pardoen, T., and Hutchinson, .J W.**: An extended model for void growth and coalescence, *Journal of the Mechanics and Physics of Solids*, 48, 2467–2512, **2000.**

[19] **Gologanu, M., Leblond, J B., Perrin, G., and Devaux J.**: Theoretical models for void coalescence in porous ductile solids. I. Coalescence "in layers", *International Journal of Solids and Structures*, 38, 5581–5594, **2001.**

[20] **Koplik, J., and Needleman, A.**: Void growth and coalescence in porous plastic solids, *International Journal of Solids and Structures*, 24, 835–853, **1988.**

[21] **Klocker, H., Tvergaard, V.**: Void growth and coalescence in metals deformed at elevated temperature, *International Journal of Fracture*, 106, 259–276, **2000.**

[22] **Duvan, H., Carlos, M., and Xianmin, X.**: A numerical study of void coalescence and fracture in nonlinear elasticity, *Computer Methods in Applied Mechanics and Engineering*, 303, 163–184, **2016.**

[23] **Keralavarma, S. M., Hoelscher, S., and Benzerga, A. A.**: Void growth and coalescence in anisotropic plastic solids, *International Journal of Solids and Structures*, 48, 1696–1710, **2011.**

[24] **Yerra, SK., Tekoglu, C., Scheyvaerts, F., Delannay, L., Van Houtte, P., and Pardoen, T.**: Void growth and coalescence in single crystals, *International Journal of Solids and Structures*, 47, 1016–1029, **2010.**

[25] **Brocks, W., Sun, DZ., and Honig, A.**: Verification of the transferability of micromechanical parameters by cell model calculations with viscoplastic materials, *International Journal of Plasticity*, 11, 971–989, **1995.**

[26] **Hom, CL., and McMeeking, M.**: Void growth in elastic–plastic materials, *ASME Journal of Applied Mechanics*, 56, 309–317, **1989.**

[27] **Worswick, M., and Pick, R.**: Void growth and constitutive softening in a periodically voided solid, *Journal of the Mechanics and Physics of Solids*, 38, 601–625, **1990.**

[28] **Richelsen, AB., and Tvergaard, V.**: Dilatant plasticity or upper bound estimates for porous ductile solids, *Acta Metallurgica and Materialia*, 8, 2561–77, **1994.**

[29] **Kuna, M., and Sun, DZ.**: Three-dimensional cell model analyses of void growth in ductile materials, *International Journal of Fracture*, 81, 235–258, **1996.**

[30] **Siad, L., Ould Ouali, M., and Benabbes, A.**: Comparison of explicit and implicit finite element simulations of void growth and coalescence in porous ductile materials, *Materials and Design*, 29, 2, 319–329, **2008.**

[31] **Sun, DZ., and Honig, A.**: Micromechanics of coalescence in ductile fracture, *International Journal of Plasticity*, 99, 2–15, **1995.**

[32] **Nahshon, K., and Hutchinson, J.**: Modification of the Gurson model for shear failure, *European Journal of Mechanics,* 27, 1, 1–17, **2008.**

[33] **Wen, J., Huang, Y., Hwang, K., Liu, C., and Li, M.**: The modified Gurson model accounting for the void size effect, *International Journal of Plasticity*, 21, 2, 381–395, **2005.**

[34] **Needleman, A., and Tvergaard, V.**: An analysis of ductile rupture in notched bars, *Journal of the Mechanics and Physics of Solids*, 32, 6, 461–490, **1984.**

[35] **Chu, C., and Needleman, A.**: Void nucleation effects in biaxially stretched sheets. *ASEM Journal of Engineering Materials and Technology*, 102, 3, 249-256, **1980.**

[36] **Benzerga, A. A., and Leblond, J.**: Ductile Fracture by Void Growth to Coalescence, *to appear in Advances in Applied Mechanics*, **2010.**

[37] **Pardoen, T., Doghri, I., and Delannay, F.**: Experimental and numerical comparison of void growth models and void coalescence criteria for the prediction of ductile fracture in copper bars, *Acta Materialia*, 46, 541–552, **1998.**

[38] **Kim, J., Gao, X., and Srivatsan, T. S.**: Modeling of void growth in ductile solids: effects of stress triaxiality and initial porosity, *Engineering Fracture Mechanics*, 71, 379–400, **2004**.

[39] **Yang, Z., and Zengtao, C.**: On the effect of stress triaxiality on void coalescence, *International Journal of Fracture,* 143, 105–112, **2007.**